REPORT
DM - 52
OCTOBER 1990

ATMOSPHERIC WATER PARAMETERS IN MID-LATITUDE CYCLONES OBSERVED BY MICROWAVE RADIOMETRY AND COMPARED TO MODEL CALCULATIONS

Kristina B. Katsaros, Ulla Hammarstrand and Grant W. Petty

DEPARTMENT OF METEOROLOGY
UNIVERSITY OF STOCKHOLM

INTERNATIONAL METEOROLOGICAL
INSTITUTE IN STOCKHOLM

ISSN 0349 - 0467

DEPARTMENT OF METEOROLOGY
STOCKHOLM UNIVERSITY (MISU)

REPORT DM-52
1990-10-25

INTERNATIONAL METEOROLOGICAL
INSTITUTE IN STOCKHOLM (IMI)

Arrhenius Laboratory
S-106 91 STOCKHOLM, Sweden
Phone 08-16 20 00

ATMOSPHERIC WATER PARAMETERS IN MID-LATITUDE CYCLONES OBSERVED BY MICROWAVE RADIOMETRY AND COMPARED TO MODEL CALCULATIONS

by Kristina B. Katsaros and Grant, W. Petty, Dept. of Atmospheric Sciences, University of Washington, Seattle, USA

Ulla Hammarstrand, Department of Meteorology, Stockholm University, Stockholm, Sweden

original contains color illustrations

ABSTRACT

This report covers exploratory work applying existing and experimental algorithms for various parameters of atmospheric water content (integrated water vapor, cloud water, precipitation and precipitation size ice particles) to signals from the Special Sensor Microwave Imager (SSM/I) to examine the distribution of these quantities in mid-latitude cyclones. We also present two cases where the older microwave radiometer, Nimbus Scanning Multichannel Microwave Radiometer (SMMR) for North Atlantic cyclones are compared to the precipitation and water vapor content from the mesoscale numerical model of the University of Stockholm (as of 1983). Our objective is to illustrate the *potential* microwave remote sensing has for enhancing our knowledge of the horizontal structure of these storms and to aid the development and testing of the cloud and precipitation aspects of limited-area numerical models of cyclonic storms. The work was originally presented at the Palmén Memorial Symposium in Helsinki, Finland, August 29-September 2, 1988.

CONTENTS

		Page
1.	Introduction	2
2.	Microwave sensors and retrieval algorithms	4
	2.1 SMMR	5
	2.2 SSM/I	6
3.	The Numerical model	8
4.	Results: Mesoscale structure of atmospheric water in a frontal zone with SSM/I	9
5.	Comparison between numerical model forecasts and SMMR observations of atmospheric water	15
	5.1 Cloud water and rain	15
	5.2 Integrated water vapour	17
6.	Conclusions	20
7.	Acknowledgements	21
8.	References	22

1. INTRODUCTION

Some twenty five years after the possibility was first suggested, horizontal distributions of several important components of atmospheric water content -- integrated water vapor, cloud liquid water, and precipitation -- can now be routinely mapped over the ocean using microwave radiometer measurements from satellites. The two most recent instruments of this type are the Scanning Multichannel Microwave Radiometer (SMMR), which operated on the Nimbus-7 satellite from October 1978 until late 1987, and the Special Sensor Microwave/Imager (SSM/I) launched in June 1987 on a satellite in the United States Defense Meteorological Satellite Program (DMSP).

Integrated atmospheric water vapor ("precipitable water"), can be retrieved accurately from these instruments and compare well to radiosonde data (e.g., Katsaros et al. 1981, Alishouse 1983, McMurdie 1989, Petty and Katsaros 1990c). Such water vapor retrievals have been used for inferring synoptic frontal locations and for investigating certain aspects of cyclone structure and kinematics (e.g., McMurdie and Katsaros 1985, Katsaros and Lewis 1986, McMurdie et al. 1987, Katsaros et al. 1989).

Algorithms for calculating cloud water and rain rate, on the other hand, are the subject of ongoing research. The validation of cloud liquid water and rain rate algorithms over the ocean is complicated by the limited availability of comparison data. Also, because of the long wavelengths employed on microwave sensors and the practical limitations placed on antenna size in space, the spatial resolution of these instruments is still marginal for mapping details of phenomena such as very narrow frontal rainbands and individual convective clouds which do not fill the antenna beam.

Despite present limitations, observations by satellite microwave radiometers of atmospheric water allow new insight into the mesoscale structure of midlatitude cyclones. In the past, visible and infrared satellite pictures have given valuable qualitative information on distributions of cloudiness and likely locations of precipitation, but microwave radiometry promises a more quantitative picture of these parameters. Microwave techniques directly

measure the vertically integrated water content of the whole atmosphere, as opposed to cloud top parameters observed by visible and infrared sensors, and they are unaffected by the extensive cirrus shield which frequently accompanies midlatitude frontal cloud bands and other weather systems.

Numerical modelers have long been expressing a desire for quantitative cloud data for intercomparison with their water parameterizations. Not only are the location and rate of production of liquid water of meteorological interest in their own right, but the skill of a model in forecasting these parameters is a sensitive measure of the correctness of both the initialization and the simulated dynamics. Furthermore, in higher resolution mesoscale models and in models forecasting over longer time periods, the dynamics are themselves sensitive to the rates of latent heat release due to condensation and to the radiative heating or cooling which occurs in the presence of clouds. Before the advent of microwave radiometry from space, direct large scale measurements of integrated cloud water were unobtainable over the ocean in any form.

In this note we demonstrate the unique ability of microwave radiometry to:

(a) provide mesoscale maps of cloud water and precipitation distributions in cyclones, and,

(b) provide independent verification of the reasonableness of atmospheric water parameters produced by a limited area numerical model (Hammarstrand, 1987).

Since currently neither model parameterizations nor satellite algorithms for cloud water or rain are well established, these qualitative intercomparisons are expected to stimulate and aid developments in both areas of research. We first give a short description of the two microwave radiometers and the algorithms we have used (Section 2). These algorithms are still undergoing development and refined revisions will be published in the near future (Petty, 1990). In Section 3 the numerical model is described and the limitations of the current study due to evolving computer systems is presented. In Section 4 we illustrate

atmospheric water, as vapor, cloud water, and precipitation size ice within midlatitude cyclones. Section 5 presents a somewhat mismatched, yet indicative, comparison between satellite observed cyclonic systems and parameters produced by the numerical model. In Section 6 we present suggestions for further work.

2. MICROWAVE SENSORS AND RETRIEVAL ALGORITHMS

The characteristics of the two microwave radiometers are given in Table 1. The SMMR is described by Gloersen and Barrath (1977), and the SSM/I by Hollinger et al. (1987).

Microwave techniques for retrieving atmospheric parameters work best over the ocean, because the ocean has low, relatively uniform emissivity ($\varepsilon \sim 0.5$) and therefore provides a good background for observing atmospheric emission.

Table 1. Characteristics of the Two Polar Orbiting Radiometers - SMMR on Seasat and on Nimbus 7 and the SSM/I on the F8 DMSP Satellite

SMMR		SSM/I	
FREQ. GHz	APPROX. RESOLUTION (km)	FREQ. GHz	APPROX. RESOLUTION (km)
6.6	150	--	--
10.7	100	--	--
18	65	19.35	55
21	60	22.235	50
37	35	37	35
--	--	85.5	15
Swath Width:		*Swath Width*:	1400 km
Seasat:	650 km		
Nimbus 7:	780 km		
Period of Operation:		*Period of Operation:*	
Seasat:	July-October 1978	July, 1987 - Present	
Nimbus 7:	October 1978-Fall, 1987		

2.1 SMMR

The algorithms used here for calculating SMMR integrated water vapor are linear combinations of the brightness temperatures obtained from selected radiometer channels. We used the coefficients developed by the Nimbus-7 Experiment Team (User's Guide for the Nimbus-7 SMMR PARM and MAP tape, 1983) based on the work of Staelin et al. (1976), Rosenkranz et al. (1978) and Chang and Wilheit (1979). Water vapor values derived from the Nimbus 7 SMMR have been found to give rms error values of the order of 2 kg m^{-2} (e.g., McMurdie, 1989).

Integrated cloud liquid water (ICLW) was determined from the SMMR data using the normalized 37 GHz polarization difference to estimate cloud optical depth, as discussed by Petty and Katsaros (1990a). In contrast to the histogram method described in that study, however, "clear sky" polarization differences were estimated here based on co-located SMMR water vapor and wind speed retrievals combined with a preliminary version of the theoretical brightness temperature model described by Petty (1990). Conversion of cloud opacities to ICLW was accomplished using the liquid water extinction formula given by Petty (1990), assuming a mean cloud temperature of 273 K.

It is very difficult to reliably separate the ICLW signal from the rain signal. Here, we simply assume that values returned by the ICLW algorithm which are less than 0.5 kg m^{-2} are due solely to cloud water and are thus quantitatively reliable; retrieved values greater than 0.5 kg m^{-2} are considered to be du: at least in part, to rain of unknown intensity. This threshold, while somewhat arbitrary, found to work reasonably well in practice, as non-precipitating clouds are rarely expected to support such large ICLW values averaged over the 30 km footprint of the SMMR, while precipitation, because of the larger effective layer depth and the proportionally stronger microwave extinction by precipitation size

drops, typically gives rise to 37 GHz polarizations which are interpreted by the ICLW algorithm as being due to ICLW well in excess of 1 kg m^{-2}.

2.2 SSM/I

The algorithms used here to retrieve integrated water vapor, integrated cloud liquid water, and indices of precipitation from SSM/I brightness temperatures are documented in detail by Petty and Katsaros (1990c). The integrated water vapor (IWV) algorithm is based on statistical regression of functions of SSM/I 19 and 22 GHz brightness temperatures against 515 coincident radiosonde estimates of IWV. The IWV estimates are obtained at 50 km resolution and are further smoothed using a 75 km averaging window in order to reduce pixel-scale noise. RMS relative differences between radiosonde and SSM/I estimates of IWV were found to be about 13%, of which a significant (but unknown) fraction of this difference is likely to be due to errors in the radiosonde estimates themselves and to spatial and temporal mismatches.

Integrated cloud liquid water (ICLW) is obtained using a semi-physical approach. SSM/I observations of surface wind speed and IWV (using the lower resolution channels) are used to estimate the cloud-free polarization difference at 85 GHz; the ratio of the observed 85 GHz polarization difference to this cloud-free polarization difference, which we refer to as the *normalized polarization difference* P_{85}, is a simple function of the total cloud water. Fields of ICLW are thus obtained at 15 km resolution, with absolute uncertainties of the order of 0.05 kg m^{-2}.

A similar approach is used to obtain the normalized 37 GHz polarization difference P_{37}, which Petty and Katsaros (1990a, 1990b) showed to be a useful index of the presence and intensity of precipitation due to the latter's effect on the visibility of the highly polarized sea surface. Values of P_{37} from 0.9 to 1.0 appear to reliably rule out rain within the pixel;

$P_{37} < 0.8$, on the other hand, may be taken as a fairly unambiguous indication of rain, with values of P_{37} decreasing to near zero with increasing intensity and areal extent of precipitation within each 25 km SSM/I pixel.

At 85 GHz, radiative scattering by precipitation-size ice particles (i.e., graupel, hail, snow aggregates) above the freezing level gives rise to a brightness temperature signal which is significantly depressed compared with brightness temperatures under otherwise similar conditions of atmospheric opacity. Our algorithm for detecting this effect, expressed here as a *polarization corrected brightness temperature depression* S_{85} (referenced to 273 K), is a slightly modified version of the one developed by Spencer et al. (1989); the principal difference is that our version automatically adjusts for variations in the oceanic and atmospheric background in order to reduce spurious variations in S_{85} arising from factors other than precipitation.

The concentrations of large ice particles required to give $S_{85} > 10$ K appear to occur primarily in conjunction with the heavier, cold-cloud rainfall associated with convective activity or intense midlatitude frontal rain bands. Preliminary comparison to radar measurements (e.g., Petty and Katsaros, 1989) show that, within a given midlatitude storm, the 85 GHz scattering signal is highly correlated with surface rainfall intensity within the SSM/I pixel. The exact statistical relationship, however, appears to vary somewhat from time to time and place to place, owing to its dependence on the details of the cloud microphysics and other factors.

Unlike other atmospheric parameters derived from SSM/I observations S_{85} appears to work equally well for identifying precipitation over land, except in the presence of surface snow cover, which also gives rise to a strong scattering signal.

3. THE NUMERICAL MODEL

A parameterization scheme for the forecast of liquid water, precipitation and cloud cover was developed at the University of Stockholm, Sweden (Sundqvist, 1978, 1981; Hammarstrand, 1987). It is designed to be included in a large numerical weather prediction model. At present the scheme, in a somewhat modified version, is used in the forecast models of the University of Bergen, Norway (Sundqvist et al., 1989) and at the Norwegian Weather Service in Oslo (Nordeng, 1986). In this scheme, stratiform and convective condensation processes are treated separately. Rain rate is parameterized in terms of cloud water contents for each category, and the total precipitation is the sum of the stratiform and convective components.

The present study makes use of results from experiments with the scheme incorporated in a limited area model (LAM) version of the European Centre for Medium Range Weather Forecasts (ECMWF) global gridpoint model. Integrations were carried out for 36 hour periods, using operational ECMWF initialization data from a week in May, 1983. Output from the model forecasts included, among other meteorological parameters, accumulated precipitation, total cloud cover, integrated cloud liquid water and water vapor. Cases for comparison were selected based on geographical and temporal coincidence of the available data with overpasses by the Nimbus 7 SMMR. Despite the non-optimality for SMMR comparison purposes of some of the times and parameters available from the model*, we

* When the present experiments were undertaken we were not aware of the possibilities of comparing the results with the SMMR data. The output from the model was therefore not chosen to coincide in time and character with the output from SMMR. For example, we chose to plot accumulated precipitation for the period of integration, but the precipitation parameter available from SMMR is the instantaneous distribution of precipitation. The experiments should therefore have been rerun, but this was not possible due to the installation of a new computer system; unfortunately, the LAM was not easily converted to the new system.

believe that our results are valuable since they show weak points in the model formulation that can be adjusted when new experiments are undertaken. Furthermore, our comparisons show a new way to verify model outputs that have not been used before.

4. RESULTS: MESOSCALE STRUCTURE OF ATMOSPHERIC WATER IN A FRONTAL ZONE WITH SSM/I

Fig. 1 depicts the 0600 UTC surface analysis of a mature cyclone moving into the British Isles on the morning of 18 October 1987. At this time, the cold front extended from the Irish Sea southwestward, with a frontal wave analyzed some 400 km northwest of the Iberian Peninsula. The exact position and amplitude of the wave was uncertain, owing to the sparsity of surface reports in the vicinity.

Fig. 2 shows the NOAA-10 infrared image of the same storm at 0420 UTC. The circulation around the low pressure center is evident west of Ireland, as is an extensive cirrus shield accompanying most of the occluded front and the upper portion of the cold front and wave. Behind the cold front, considerable open-cell convection is visible, including a region of stronger, more organized convection near 20°W, 47°N which is apparently associated with the secondary low seen in the surface analysis.

Fig. 3 depicts composite SSM/I views of the cyclone from 0445 UTC (eastern swath) and 0620 UTC (overlapping western swath), using the algorithms described in Sect. 2. The cirrus shield seen in the infrared image (Fig. 2) is transparent to microwaves and is therefore invisible in the SSM/I images.

The SSM/I integrated water vapor image (Fig. 3a) exhibits the characteristic water vapor maximum in the warm air sector ahead of the cold front, accompanied by a sharp decrease across the front in the direction of the cold air mass, as documented by McMurdie and Katsaros (1985) in

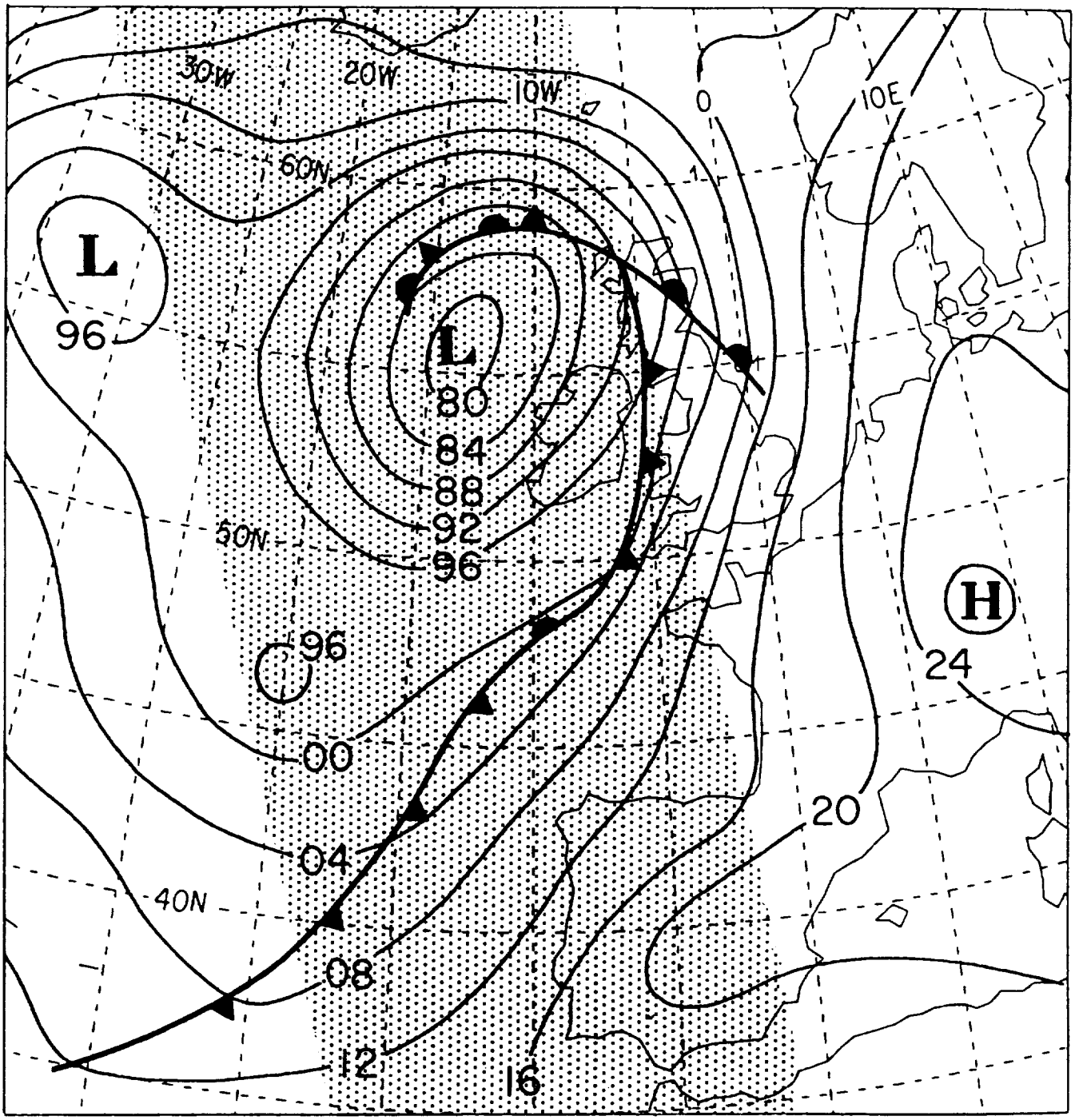

Figure 1: Surface analysis of an occluded cyclone overrunning the British Isles, valid 06 UTC, 18 October 1987.

Figure 2: NOAA-10 infrared image, 0420 UTC, 18 October 1987, produced at University of Dundee, Scotland.

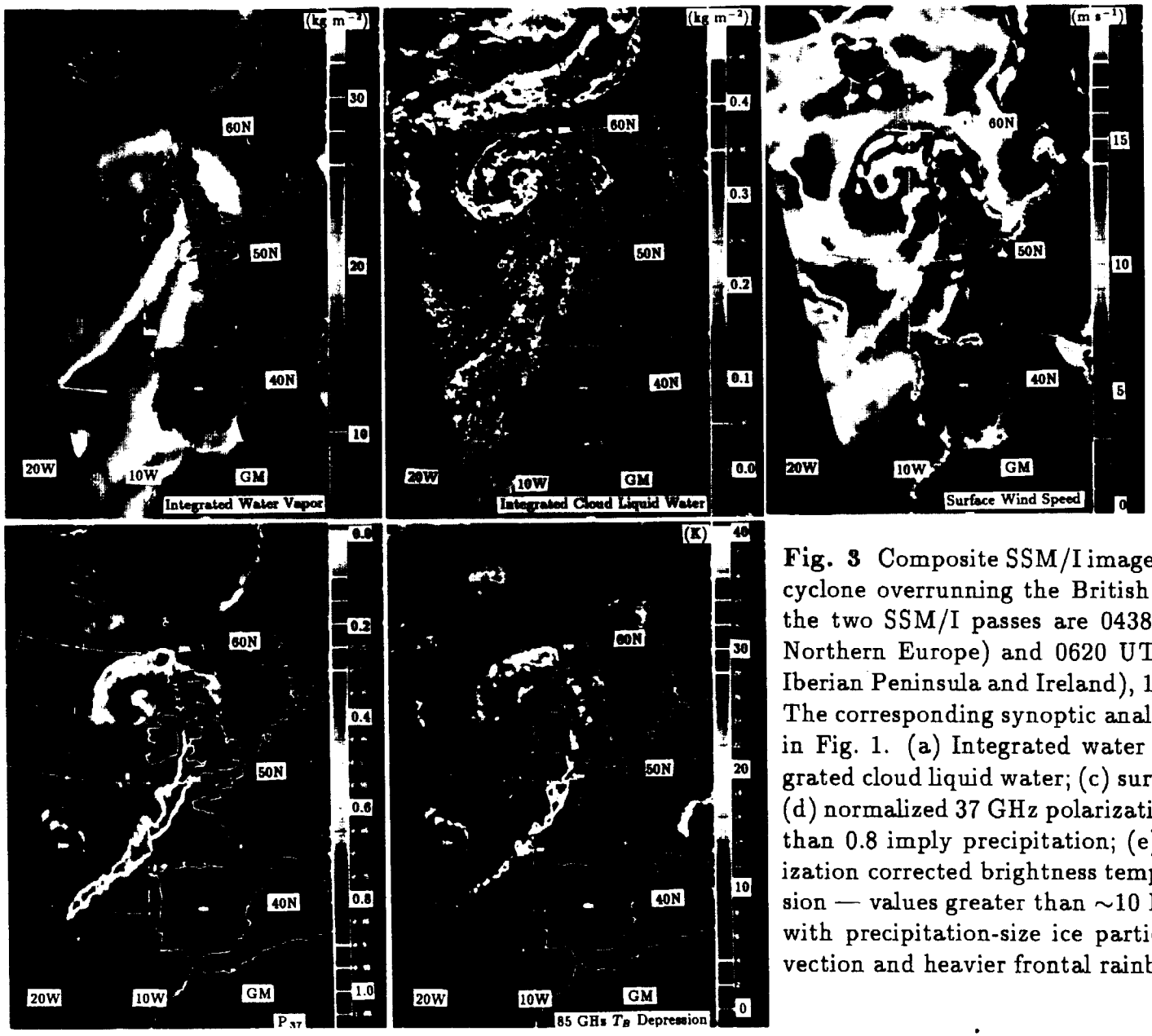

Fig. 3 Composite SSM/I images of an occluded cyclone overrunning the British Isles. Times of the two SSM/I passes are 0438 UTC (crossing Northern Europe) and 0620 UTC (crossing the Iberian Peninsula and Ireland), 18 October 1987. The corresponding synoptic analysis is presented in Fig. 1. (a) Integrated water vapor; (b) integrated cloud liquid water; (c) surface wind speed; (d) normalized 37 GHz polarization — values less than 0.8 imply precipitation; (e) 85 GHz polarization corrected brightness temperature depression — values greater than ~10 K are associated with precipitation-size ice particles within convection and heavier frontal rainbands.

SMMR data. In a recent study (Katsaros et al. 1989), we have found that the location of SSM/I water vapor gradients exceeding 0.1 (kg m^{-2})/km provides an excellent objective indication of the location of many surface cold fronts, irrespective of latitude and season. Note that there is no obvious indication in the water vapor field of the frontal wave that had been analyzed northwest of the Iberian Peninsula (Fig. 1).

The liquid water image (Fig. 3b) shows a detailed map of the vertically integrated liquid water content of the atmosphere, many features of which bear little apparent relation to the infrared brightness temperatures seen in Fig. 2 (because of the time elapsed between the SSM/I swaths and the infrared image, only general comparisons are meaningful). For example, the extensive layer of stratus northeast of Iceland appears very uniform in the infrared image, yet the SSM/I reveals significant variations in the total water content of these clouds, with maxima near 0.4 kg m^{-2}. The strong SSM/I liquid water signal just south of Iceland appears to be associated with low clouds which are barely discernible in the infrared image because of the intervening cirrus layer. Blacked out pixels are those for which precipitation has been flagged, based on $S_{85} > 10$ K. Numerous cold air mass convective cells are evident behind the cold front; most of these appear to have pixel-averaged liquid water contents of less than 0.2 kg m^{-2}.

The SSM/I derived surface wind speed field, which is used as an input in the calculation of the atmospheric water fields, is depicted in Fig. 3c. In general, the wind speed field is in good agreement with the pressure gradient field in the conventional surface analysis. A single obvious exception occurs near the south coast of Iceland, where the relatively high wind speeds retrieved by the SSM/I would seem to support a tighter packing of the isobars toward Iceland and a weaker gradient midway between Iceland and the occluded front. Note that some of the relatively high wind speeds indicated in the immediate vicinity of the frontal cloud band may be due to contamination of the wind signal by precipitation.

Fig. 3d depicts the normalized 37 GHz polarization difference P_{37}, a measure of the visibility of the polarized sea surface through clouds and precipitation. As indicated in section 2, values of P_{37} below 0.8 are taken to correspond to precipitation. A narrow, well-defined band of precipitation is seen along the entire length of the front, including the occluded portion wrapping around the low center near 55N, 13W. Some mesoscale structure in the form of kinks and local enhancements in the rainband is evident , particularly west of France. However, if one assumes that the shape and location of the precipitation band are mainly determined by the location of the surface cold front, then there would again appear to be little evidence of the pronounced frontal wave analyzed in Fig. 1. Although we did not have access to the conventional reports used in the synoptic analysis, it may be questioned whether the surface cold front would have been analyzed with this wave, had the SSM/I images of water vapor and precipitation been available to the analyst.

Fig. 3e depicts the polarization-corrected depression (S_{85}) of the 85 GHz brightness temperature. Values departing greatly from zero are associated with strong radiative scattering due to precipitation-size ice within convective clouds and frontal rainbands. Despite the use of the same 85 GHz channels for both S_{85} and for the liquid water field (Fig. 3b), the two fields are seen to be quite different. For example, The significant liquid water features observed north of 60°N latitude in Fig. 3b have little or no associated scattering signal. This is consistent with our identification of that region of liquid water with low, stratiform clouds in which vertical motions are weak and the formation of significant concentrations of large ice particles is unlikely. Certain portions of the spiral cloud band near 55°N also show relatively high liquid water content but little to no scattering by ice. Likewise, the majority of the cellular cloudiness evident behind the cold front in both the infrared and liquid water images also exhibits no scattering signal. Those few cells which are also evident in Fig. 3b are apparently associated with well developed cumulonimbus clouds capable of producing large graupel and perhaps even hail aloft.

Of greatest interest, of course, are the well-defined regions of precipitating ice appearing within the frontal cloud band itself. Although they appear almost exclusively within those regions identified as precipitating in Fig. 3d, the scattering signal provides considerable additional meso-α scale information concerning the locations and relative intensities of precipitation activity along the front. For example, individual precipitation cores with diameters of less than 30 km appear to be easily resolvable within the southern end of the frontal rain band. The structure and strength of features in the SSM/I ice-scattering imagery have been found in other cases to closely match the structure and intensity of coincident surface radar echoes (Petty and Katsaros, 1989).

5. COMPARISON BETWEEN NUMERICAL MODEL FORECASTS AND SMMR OBSERVATIONS OF ATMOSPHERIC WATER

5.1 Cloud water and rain

Two passes of the Nimbus 7 satellite measuring rain and cloud associated with waves on the polar front are presented in Fig. 4. The frontal analysis was obtained from the German Weather Service (Deutsche Wetterdienst) and contours represent accumulated precipitation (in mm) calculated by the model for the period 00 UTC to 18 UTC on 23 May 1983. The plotted symbols represent SMMR-derived ICLW values, obtained from satellite passes at 1218 UTC and 1358 UTC on the same date. In several regions values exceeding 0.5 kg m^{-2} appear. We interpret these as occurrence of rain of unknown intensity. The position and shape of the SMMR-observed rain pattern near 45°W suggest that the cold frontal position obtained from the operational German surface should be advanced by about 200 km and oriented more North-South.

The model-derived convective precipitation region (near 52N, 20°W) is centered on a band of heavy cloud water and rain observed by the SMMR. The SMMR also finds significant precipitation in other areas along the front, both to the north and to the south, where the model failed to predict any accumulation. West of 40°W, both the model and the SMMR

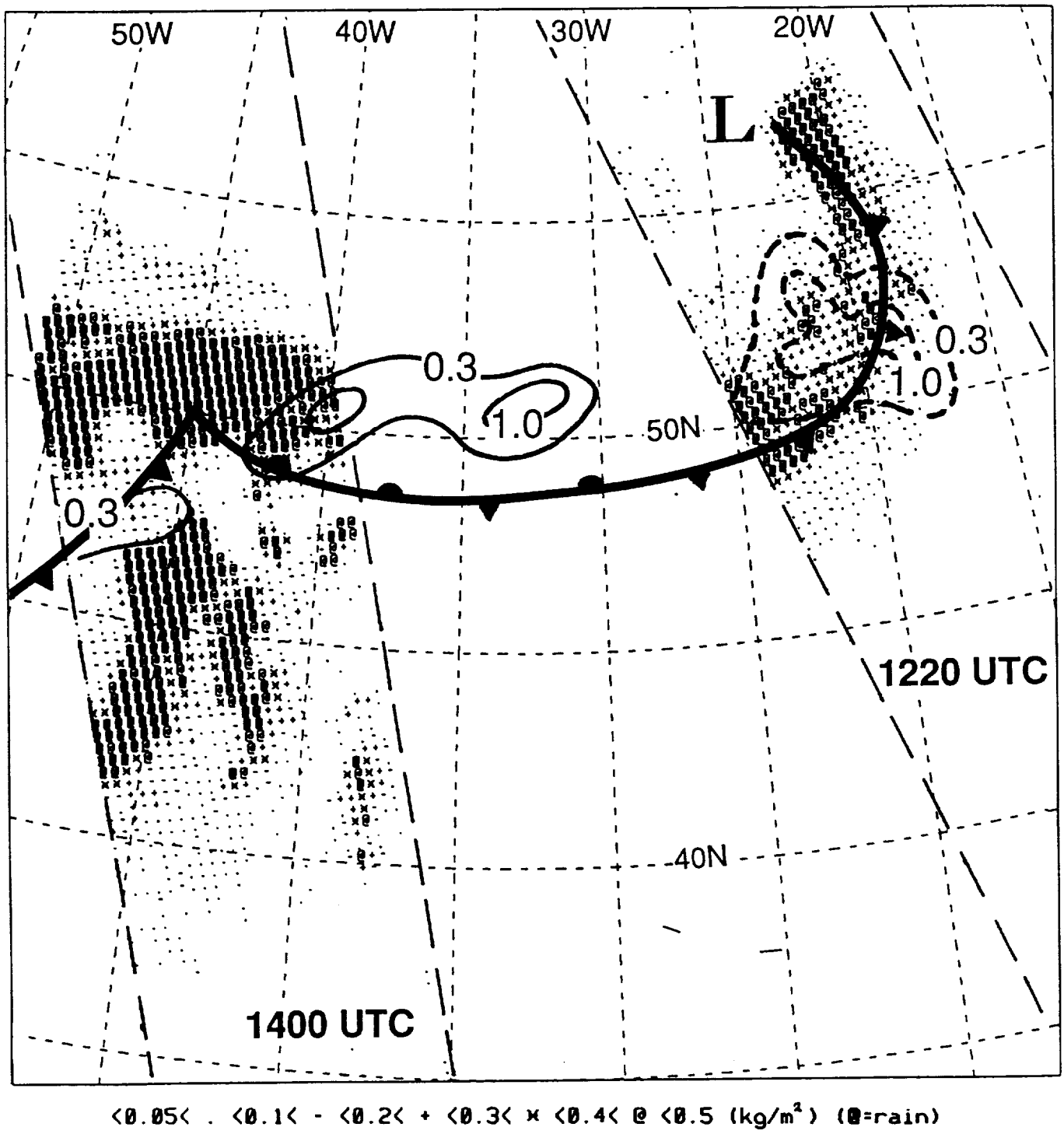

Figure 4: SMMR inferred integrated liquid water content observed over the North Atlantic at 1220 UTC (right swath) and 1400 UTC (left swath), 23 May 1983, compared with accumulated precipitation (mm) predicted by limited-area model for period 00 UTC - 18 UTC, 23 May. Values of SMMR ILWC > 0.5 kg m^{-2} are interpreted as rain of unknown intensity. Solid contours represent stratiform precipitation predicted by the model; dashed contours represent convective precipitation. Frontal positions were taken from the *Berliner Wetterkarte* for 12

identify areas of precipitation associated with an open-wave cyclone. Again, the SMMR-observed rain field is considerably more extensive than that predicted by the model. Similar results are seen in Fig. 5, which depicts non-frontal stratiform rain associated with a low pressure center west of Norway.

The difference between the predicted and the observed distributions of rain may be due to a number of factors. For example, the model's parameterized condensation and/or rate of conversion to rain may be too slow, or the model may have underestimated the convergence field in these cyclones.

5.2 Integrated Water Vapor

Figure 6a depicts the patterns of integrated water vapor observed by the SMMR at 0137 UTC, 21 May 1983. The data swath sampled an area in advance of a weak cold front approaching from the west. Fig. 6b depicts the model's 36-hour forecast of integrated water vapor for the same area, valid at 0600 UTC, 21 May 1983, or approximately 4.3 hours following the SMMR pass.

Both the patterns and the magnitude of the two fields agree remarkably well in the region east of 20°,0°)W. West of 20°W, the model forecast is significantly moister than the field observed by the SMMR. Given the time delay, it is possible that moisture advected into the region under the influence of the approaching front is partly responsible for the increase. However, the rate of advection and/or convergence necessary to bring about such a change in only four hours seems unreasonably large. It is more likely that the model is simply carrying too much water vapor ahead of the front, which may result from inefficiencies in the parameterization of condensation and release of precipitation. This assumption is supported by the results from Fig. 4 and 5 discussed above.

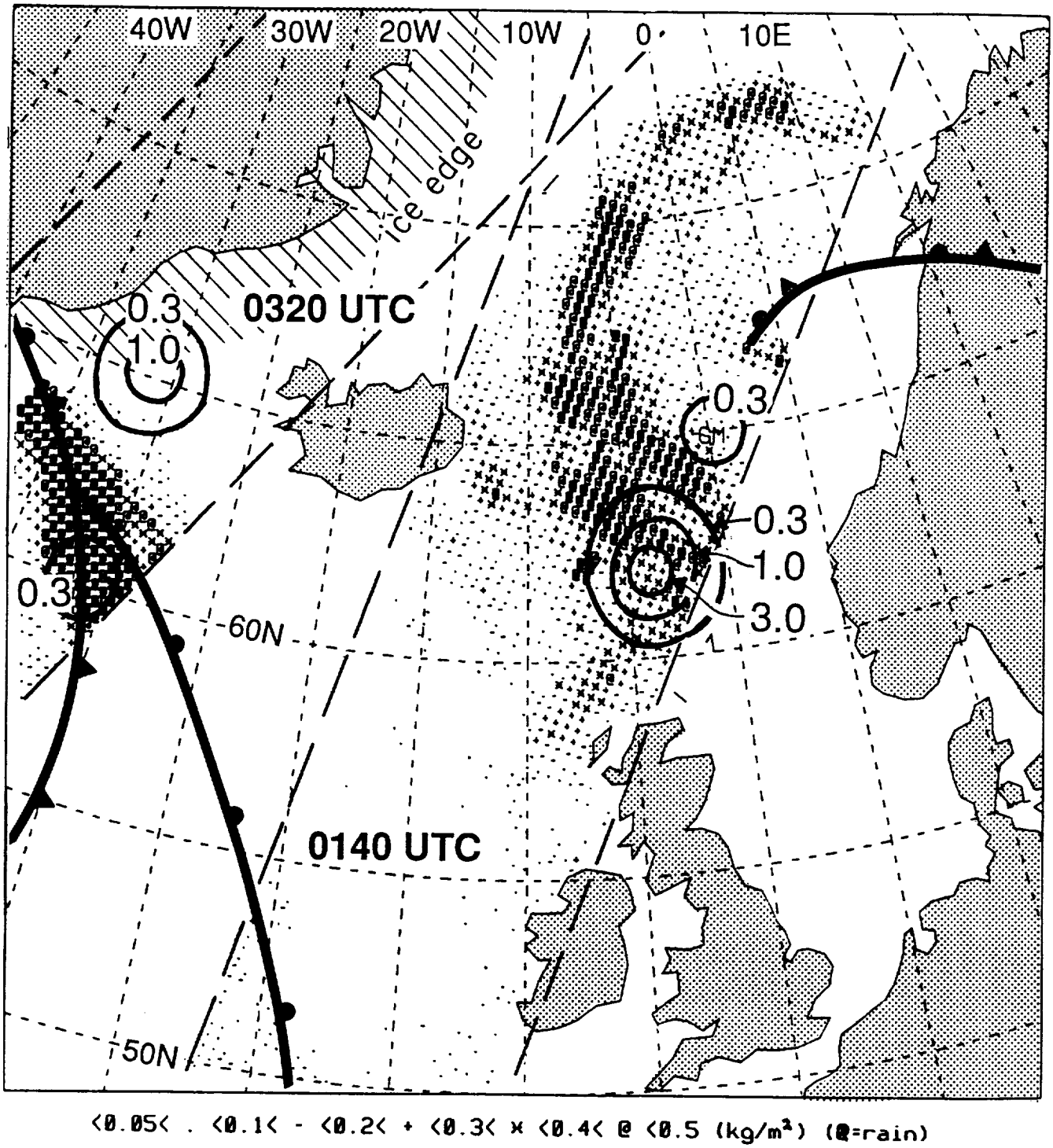

Figure 5: SMMR inferred integrated liquid water content observed over the North Atlantic at 0140 UTC (right swath) and 0320 UTC (left swath), 21 May 1983, compared with accumulated precipitation (mm) predicted by limited-area model for period 00 UTC - 18 UTC, 23 May. Values of SMMR ILWC > 0.5 kg m^{-2} are interpreted as rain of unknown intensity. Solid contours represent stratiform precipitation predicted by the model. Frontal positions were taken from the *Berliner Wetterkarte* for 00 UTC.

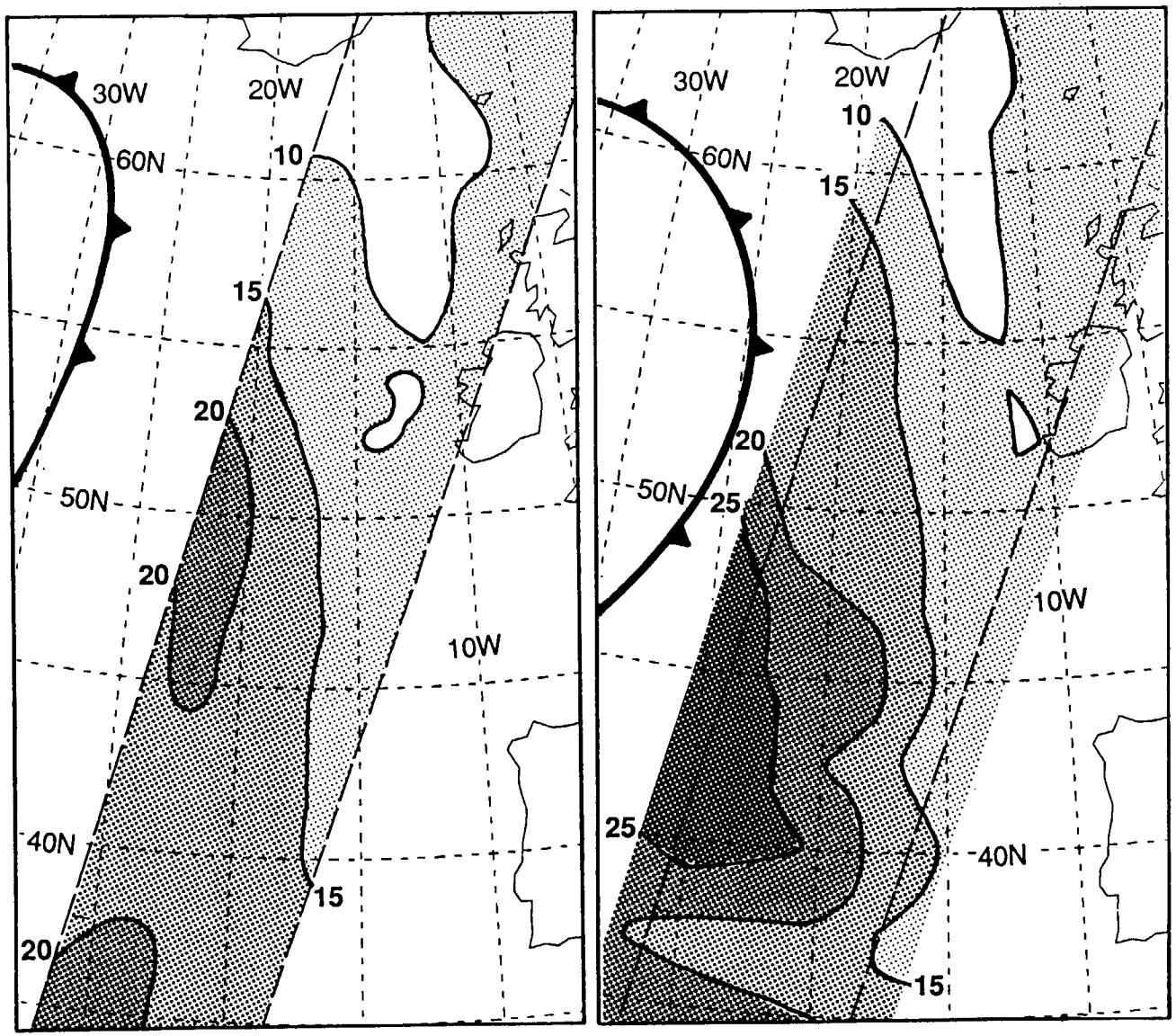

Figure 6: Comparison between SMMR-observed and model-predicted integrated water vapor fields over the North Atlantic.

a) SMMR integrated water vapor (kg m^{-2}) observed at 0140 UTC, 21 May 1983. Frontal position valid 00 UTC, 21 May 1983.

b) 36-hour forecast of integrated water vapor (kg m^{-2}) by limited-area model, valid 06 UTC, 21 May 1983. Frontal position valid 06 UTC.

Water vapor fields produced in the model are influenced by a number of factors, including the initialization, the parameterization of vapor source and sink terms (e.g., surface fluxes and condensation processes), and the calculated horizontal and vertical motion fields. This comparison suggests that, at least for the case described here, one or more of these factors may require some adjustment in the model. Comparisons using a larger set of model predictions and coincident microwave radiometer observations could be very useful in isolating and quantifying such errors.

6. CONCLUSIONS

With this short report we wish to draw attention to the valuable resource for observing the mesoscale structure of midlatitude cyclones that microwave radiometers operating from space provide. The high spatial resolution and unique properties of the SSM/I 85 GHz channels make them a particularly welcome addition to existing satellite tools. Rainbands and regions of embedded convection within frontal clouds appear to be directly detectable at resolutions never before possible from space.

The preliminary comparisons between a limited-area model and SMMR data show that microwave sensors in space can potentially be used to provide much needed comparison data for atmospheric liquid water and water vapor parameterizations in numerical forecast models.

Microwave radiometer observations should also be used to improve the initial water vapor fields for the numerical forecast models. When the predicted fields of clouds and precipitation are tested against microwave observations it would then be a better test of the model's performance. Since these microwave radiometers only provide integrated values of the atmospheric water parameters, the satellite measurements would have to be used as a

constraint and the models distribution of the water vapor in the vertical would have to be employed.

Even though the present comparison between hydrologically important parameters measured by microwave radiometers and similar quantities predicted by numerical models is only qualitative, it gives confidence in both types of information and suggests that it may be worthwhile to make such comparisons routinely.

7. ACKNOWLEDGMENTS

We are grateful to Erika Francis and Frank J. Wentz of Remote Sensing Systems, Inc. who generously provided the SSM/I data tapes. SMMR data tapes were obtained from the National Space Science Data Center. NOAA-10 imagery was obtained from the University of Dundee Satellite Station. The SSM/I brightness temperature and coincident radiosonde data set used to derive Eq. (1) was generously made available by Dr. John Alishouse of NOAA/NESDIS. We thank Ms. Kay Dewar for assistance with Figures 1, 4, 5 and 6, and Ms. Janet Meadows for finalizing the manuscript. This work was supported by NASA grant NAG 5-943.

8. REFERENCES

Alishouse, J.C., 1983: Total precipitable water and rainfall determination from the Seasat Scanning Multichannel Microwave Radiometer (SMMR). *J. Geophys. Res.*, **88,** 1929-1935.

Chang, A.T.C. and T.T. Wilheit, 1979: Remote sensing of atmospheric water vapor, liquid water, and wind speed at the ocean surface by passive microwave techniques from the Nimbus 5 satellite. *Radio Science,* **14,** 793-802.

Gloersen, P. and F.T. Barath, 1977: A scanning multichannel microwave radiometer for Nimbus-G and Seasat-A. *IEEE J. Ocean. Eng.*, **OE-2,** 172-178.

Hammarstrand, U., 1987: Prediction of cloudiness using a scheme for consistent treatment of stratiform and convective condensation and cloudiness in a limited area model. Collection of papers presented at the WMO/IUGG Symposium on Short and Medium Range Weather Prediction, Tokyo, 4-8 August 1986. Special Volume of the *J. Met. Soc. Japan,* 187-197.

Hollinger, J., R. Lo, G. Poe, R. Savage and J. Pierce, 1987: *Special Sensor Microwave/Imager User's Guide.* Naval Research Laboratory, Wn, D.C., 177 pp.

Katsaros, K.B., P.K. Taylor, J.C. Alishouse and J.R. Lipes, 1981: Quality of Seasat SMMR (Scanning Multichannel Microwave Radiometer) atmospheric water determinations. In *Oceanography from Space,* Gower (ed.), 691-706, Plenum Publishing Corp., New York.

Katsaros, K.B. and R.M. Lewis, 1986: Mesoscale and synoptic scale features of North Pacific weather systems observed with the Scanning Multichannel Microwave Radiometer on Nimbus 7. *J. Geophys. Res.*, **91,** 2321-2330.

Katsaros, K.B., I. Bhatti, L. McMurdie and G. Petty, 1989: Identifying Atmospheric Fronts over the Ocean with Microwave Measurements of Water Vapor and Rain. *Weather and Forecasting*, **4,** 449-460.

McMurdie, L.A. and K.B. Katsaros, 1985: Atmospheric water distribution in a mid-latitude cyclone observed by the Seasat Scanning Multichannel Microwave Radiometer. *Mon. Wea. Rev.*, **113,** 584-598.

McMurdie, L.A., G. Levy and K.B. Katsaros, 1987: On the relationship between scatterometer-derived convergences and atmospheric moisture. *Mon. Wea. Rev.*, **115,** 1281-1294.

McMurdie, L.A., 1989: *Interpretation of Integrated Water Vapor Patterns in Oceanic Midlatitude Cyclones Derived from the Scanning Multichannel Microwave Radiometer*. Ph.D. Thesis. Dept. of Atmospheric Sciences, University of Washington, Seattle, WA, 98195, USA.

Nordeng, T.E., 1986: Parameterization of physical processes in a three-dimensional weather prediction model. *Norwegian Meteorological Institute,* Technical Report No. 65, 48 pp.

Petty, G.W., 1990: *Observing the Marine Atmosphere with the Special Sensor Microwave/Imager*. Ph.D. Thesis, Department of Atmospheric Sciences, University of Washington, Seattle, WA, 98195, USA (in preparation).

Petty, G.W., and K.B. Katsaros, 1989: Empirical studies of the microwave radiometric response to precipitation in the tropics and midlatitude. Appearing in *Preprint Volume, Fourth International Conference on Satellite Meteorology and Oceanography, May 16-19, San Diego*

Petty, G.W., and K.B. Katsaros, 1990a: Precipitation observed over the South China Sea by the Nimbus 7 Scanning Multichannel Microwave Radiometer during Winter MONEX. *J. Appl. Meteor.*, **29**, 273-288

Petty, G.W., and K.B. Katsaros, 1990b: Nimbus 7 SMMR precipitation observations calibrated against surface radar during TAMEX. Submitted to *J. Appl. Meteor.* Also appearing in abbreviated form in *Preprint Volume, Fifth International Conference on Satellite Meteorology and Oceanography, September 3-7, 1990, London, England*

Petty, G.W., and K.B. Katsaros, 1990c: New geophysical algorithms for the Special Sensor Microwave Imager. Appearing in *Preprint Volume, Fifth International Conference on Satellite Meteorology and Oceanography, September 3-7, 1990, London, England*

Prabhakara, C., H.D. Chang and A.T.C. Chang, 1982: Remote sensing of precipitable water over the oceans from Nimbus 7 microwave measurements. *J. Appl. Meteor.*, **21**, 59-68.

Rosenkranz, P.W., D.H. Staelin and N.C. Grody, 1978: Typhoon June (1975) viewed by a Scanning Microwave Spectrometer. *J. Geophys. Res.*, **83,** 1857-1868.

Spencer, R.W., 1986: A satellite passive 37 GHz scattering-based method for measuring oceanic rain rates. *J. Climate Appl. Meteor.*, **25,** 754-766.

Spencer, R.W., H.M. Goodman and R.E. Hood, 1989: Precipitation retrieval over land and ocean with the SSM/I: Identification and characteristics of the scattering signal. *J. Atmos. Ocean. Tech.*,

Staelin, D.H., K.F. Kunzi, R.L. Pettyjohn, R.K.L. Poon and R.W. Wilcox, 1976: Remote sensing of atmospheric water vapor and liquid water with the Nimbus 5 Microwave Spectrometer. *J. Appl. Meteor.*, **15,** 1204-1214.

Sundqvist, H., 1978: A parameterization scheme for non-convective condensation including prediction of cloud water content. *QuartJ. Roy. Met. Soc.*, **104,** 677-690.

Sundqvist, H., 1981: Prediction of stratiform clouds: Results from a 5-day forecast with a global model. *Tellus,* **33,** 242-253.

Sundqvist, H., E. Berge and J.E. Kristjánsson, 1989: Cloud parameterization studies with a mesoscale NWP model. Report BSC 88/17, IBM Bergen Scientific Centre, 32 pp.

Users Guide for the Nimbus-7 Scanning Multichannel Microwave Radiometer (SMMR) PARM and MAP tapes, 1983. Systems and Applied Sciences Corporation, 5809 Annapolis Road, Hyattsville, MD 20784, USA, 68 pp.

DEPARTMENT OF METEOROLOGY
STOCKHOLM UNIVERSITY (MISU)

INTERNATIONAL METEOROLOGICAL
INSTITUTE IN STOCKHOLM (IMI)

Dynamic Meteorology (DM)

REPORTS

1982-

40 Hammarstrand, U., A parameterization scheme for convective cloud water and cloud cover, August 1982.

41 Nåbo, O., Combined effects of baroclinic and barotropic instability in a non-linear low order model, August 1984.

42 Sundqvist, H., Simulation of entrainment at the top of the atmospheric boundary layer for use in GCM, October 1984.

43 Johansson, Å., Theory and modelling of the interaction between sub-grid scale orography and the large scale flow, November 1984

44 Johansson, Å., On the parameterization of sub-grid scale orographic effects in models of the large scale atmospheric flow, April 1985.

45 Huang, X.-Y., A low-order model for moist convection, June 1985.

46 Carlsson, I., Theory and observations of gravity waves in an inversion layer, October 1985.

47 Hammarstrand, U. and Sundqvist, H., A consistent scheme for treatment of stratiform and convective condensation and cloudiness in numerical weather prediction models, January 1986.

48 Hammarstrand, U. and Sundqvist, H., Results from prediction of cloudiness with a limited area model, June 1986.

49 Huang, X.-Y., On the hysteretic behaviour of moist convection, February 1987.

50 Olofsson, B., A Lagrangian model of dry thermals, September 1987.

51 Bergeås, L., A bulk model for the unstable planetary boundary layer over the sea. A sensitivity investigation, April 1988.

52 Katsaros, K. B., Petty, G.W and Hammarstrand U., Atmospheric water parameters in mid-latitude cyclones observed by microwave radiometry and compared to model calculations, October 1990.

53 Gollvik, S., On applying the adjoint model technique to a time series of pressure data, October 1990.

The following report series are published at the Department of Meteorology, Stockholm University (MISU), and the International Meteorological Institute in Stockholm (IMI)

AP Atmospheric Physics

CM Chemical Meteorology (formerly Atmospheric Chemistry (AC))

DM Dynamical Meteorology

AA Atmospheric Aerosol Science

AR Annual Reports

GH Geophysical Hydromechanics ceased in 1974, last report number was GH-5.

The reports can be ordered from

Library
Department of Meteorology
Stockholm University
Arrhenius Laboratory
S-106 91 STOCKHOLM
Sweden

1 Performing organization
Stockholm University
DEPARTMENT OF METEOROLOGY
and
INTERNATIONAL METEOROLOGICAL
INSTITUTE I STOCKHOLM
Arrhenius Laboratory
S-106-91 STOCKHOLM, Sweden

☐ PROJECT DESCRIPTION 2 Acquisition number
☐ REPORT DOCUMENTATION PAGE
3 Date 4 Diary number PR

5	6	7 MI Project number
8 Project: ☐ 1 Planning ☐ 2 Amplification ☐ 3 Concluded		9 MI Report number

10	11 Contract number	12 Starting year	13 Finishing year	14 MI Report number

15 Sponsoring organization
Swedish National Science Research Council
National Aeronautic and Space administration (NASA)

16 Title and subtitle of project or report

Atmospheric Water Parameters in Mid-Latitude Cyclones Observed by Microwave Radiometry and Compared to Model Calculations.

17 Project leader/Auther(s)

Kristina Katsaros and Ulla Hammarstrand

18 Abstract (goal, method, technique, result etc.)

This report covers exploratory work applying existing and experimental algorithms for various parameters of atmospheric water content (integrated water vapor, cloud water, precipitation and precipitation size ice particles) to signals from the Special Sensor Microwave Imager (SSM/I) to examine the distribution of these quantities in mid-latitude cyclones. We also present two cases where the older microwave radiometer, Nimbus Scanning Multichannel Microwave Radiometer (SMMR) for North Atlantic cyclones are compared to the precipitation and water vapor content from the mesoscale numerical model of the University of Stockholm (as of 1983). Our objective is to illustrate the *potential* microwave remote sensing has for enhancing our knowledge of the horizontal structure of these storms and to aid the development and testing of the cloud and precipitation aspects of limited-area numerical models of cyclonic storms. The work was originally presented at the Palmén Memorial Symposium in Helsinki, Finland, August 29-September 2, 1988.

19 Abstract written by

20 Key words cloud water, precipitation, atmospheric water vapor, microwave radiometry, numerical weather prediction, mid-latitude cyclones.
21 Classification system and class(es)
UDC 551.513
22 Index terms (source)

23 Bibliographical data
Stockholm university, Department of Meteorology

24 ISSN
0349-0467
25 ISBN

26 Secret	paragraph	27 Language	28 Number of pages	29 Price
X No ☐ Yes	§ Official Secrets Act	English	25	

30 Distribution by
Library, Department of Meteorology